Propene Bulk Polymerization Kinetics: Role of Prepolymerization and Hydrogen

Jochem T. M. Pater
BP Lavéra SNC, Centre Recherche et Technologie, F-13117, Lavéra, France

Günter Weickert and Wim P. M. van Swaaij
Process Technology Institute Twente, University of Twente, High Pressure Laboratories, NL-7500AE Enschede, The Netherlands

An experimental setup for the polymerization of liquid propylene was used to carry out main polymerizations with and without a prepolymerization step. Two types of prepolymerization are introduced: at a constant temperature and at rapidly increasing reactor temperatures. With the present catalyst system, at high polymerization temperatures, a prepolymerization step will increase polymerization rate. Hydrogen was used to control the molecular weight of the product. The polymerization reactor was used in combination with a gas chromatograph to determine the vapor-liquid equilibrium (VLE) of the propylene-hydrogen system. Measurements are compared to predictions of different equations of state. The Peng-Robinson equation of state is best able to describe the VLE for this binary system. A temperature-dependent interaction parameter was derived from the fits to the measured data.

Introduction

In the past 15 years, polyolefins (PO) have shown annual growth rates of 7 to 10%. This enormous increase in the consumption of these plastics is not only due to the combination of low costs and attractive material properties, but also to the continuous broadening of the properties-window of the polyolefins, allowing replacement of other (more expensive) products by POs. Ongoing developments in catalyst research and process technology competed and pushed each other to new levels. New and improved processes require full control of kinetics, polymer, and powder morphology.

Prepolymerization

With the increase of catalyst activity over the past 20 years, the importance of the use of a prepolymerization step has increased as well to be able to maintain acceptable powder morphology and to prevent the active catalyst particles from undergoing thermal runaway. Prepolymerization is defined as a polymerization step under mild conditions, such as reduced process temperature or monomer concentration. The catalyst is normally at its highest activity in the initial stage when no deactivation has taken place and during which the catalyst particle has a small outer surface area. This combination can lead to a strong increase of particle temperature and a catalyst deactivation due to overheating. Prepolymerization can increase the particle surface area without the risk of runaway, due to low reaction rates. In addition, the prepolymerization step will allow the catalyst support material to fragment in a controlled way, without, for example, the risk of formation of undesired fines.

One of the most widely known polypropylene processes, using a prepolymerization step, is Basell's Spheripol technology. Like many other modern processes, it consists of two main polymerization steps, a homo-polymerization step in liquid propylene (PPY), and a gas-phase co-polymerization step comprising a fluidized-bed reactor. As the risk of particle overheating exists in the first reactor because of the high monomer concentrations, especially for larger catalyst particles, a liquid-phase prepolymerization step is often applied. After prepolymerization, the catalyst particles are fed to the main reactor and will have approximately the same activity per particle as the bare catalyst, but particle size will have increased by a factor of 5–10.

Although the importance of the prepolymerization step for kinetics and powder morphology is well known, only limited

Correspondence concerning this article should be addressed to G. Weickert.

data are available in open literature on these effects. This is mainly due to the difficulties in laboratory-scale experiments in liquid pool polymerization, combining the difficult nature of the experiments (very high polymerization activities and the relatively high operating pressures) with the sensitivity of the modern catalyst system for even traces of impurities. In the present work we describe a setup developed for catalytic polymerization of α-olefins in gas or liquid phase. With this hardware, a number of experimental procedures were developed to allow a prepolymerization step and powder sampling during polymerization and to be able to control process parameters like temperature, and gas and liquid composition within narrow boundaries. Moreover, most importantly, it is possible to obtain a full reaction rate vs. time curve with this method in a single experiment.

Hydrogen

An important property of the produced polymer is its molecular weight. Typically, the polyolefins show a molecular weight distribution, with a broadness determined by the type of catalyst and the process conditions during polymerization. Ziegler-Natta catalysts give significantly broader molecular weight distribution (MWD) than metallocene catalysts. The MW and MWD of the polymeric material can be described, as often mentioned in the literature, for example, by Weickert (1996a), by the propagation and termination rate constants in combination with the concentrations of the different components. Mayo derived a general description of the chain termination probability q as a function of the different propagating and terminating reaction rates

$$q = \frac{k_m}{k_p} + \frac{k_{H_2}}{k_p} \cdot \frac{C_{H_2,site}}{C_{PPY,POL}} \tag{1}$$

With all active catalyst sites showing similar behavior, the instantaneous MWD distribution can be described by the well-known Schultz-Flory distribution

$$y_j^d = j \cdot q^2 \cdot e^{-j \cdot q} \tag{2}$$

where y_j^d is the differential MWD as a function of only one parameter, the chain termination probability. However, typical ZN-catalysts show so-called multisite behavior. The different catalyst sites all have their own kinetic parameters (so the different active sites show different q-values), resulting in a polymer product having a much broader distribution than the one demonstrated in Eq. 2.

In the polymerization of propylene with a conventional Ziegler-Natta catalyst in the presence of hydrogen, chain transfer to hydrogen is the most important chain transfer mechanism. So, in modeling MW and MWD as a function of process conditions like temperature and hydrogen pressure, one needs to know $C_{H_2,site}$, the hydrogen concentration at the active catalyst center. We propose to obtain this concentration from a combination of the propylene concentration in the polymer and the hydrogen concentration in the liquid monomer. When stating that the sorbed monomer in the amorphous polymer can be considered as a liquid, we propose to calculate $C_{H_2,site}$ as the product of the mole ratio of hydrogen in the liquid propylene (L_{H_2}) and the concentration of propylene in the polymer

$$\frac{C_{H_2,site}}{M_{H_2}} = \frac{L_{H_2} \cdot C_{PPY,POL}}{M_{PPY}} \qquad (\text{kmol/m}^3) \tag{3}$$

where monomer sorption in the polymeric phase can be described as shown by Meier et al. (2001)

$$C_{PPY,POL} = \rho_{liq} \cdot \phi \qquad (\text{kg/m}^3) \tag{4}$$

where ϕ is the volume fraction of monomer, resulting from the Flory-Huggins equation

$$\ln\left(\frac{P}{P_0}\right) = \ln \phi + (1-\phi) + \chi \cdot (1-\varphi)^2 \tag{5}$$

The temperature-dependent Flory-Huggins interaction parameter χ can be determined experimentally. The mole ratio hydrogen to propylene L_{H_2} in Eq. 3 is easily calculated from the mole fraction of hydrogen in the liquid-phase X_{H_2}.

For the present system of liquid propylene and hydrogen, the availability of literature data on the vapor liquid equilibria (VLE) is limited. Williams and Katz (1954) published VLE data on some hydrogen/hydrocarbon systems. Young (1981) published a valuation of Katz's data. However, the ranges of

Table 1. Components Used in Polymerization Experiments, with their Origin, Purity and Final Treatment before Use

Component	Supplier	Purity	Further Processing
TEAL	AkzoNobel	> 96%, AlH_3 < 0.07%	none
Nitrogen	PraxAir	> 99.999%, < 4 vpm H_2O, < 4 vpm O_2, < 1 vpm CO_2	3A, 4A, 13X mole sieves, red-ed BTS cat.
Hydrogen	PraxAir	> 99.999%, < 5 vpm H_2O, < 1 vpm O_2, < 0.5 vpm CO	3A, 4A, 13X mole sieves, red-ed BTS cat.
Propylene	Prax Air	< 20 wtppm H_2O, < 5 wtppm CO_2, < 0.5 wtppm CO	3A, 4A, 13X mole sieves, ox-ed + red-ed BTS
Hexane	Merck	> 99%, < 0.01% H_2O, < 0.05% S compounds	3A, 4A, 13X mole sieves, reduced BTS cat.
D-donor	Dow Chem.		
Mole sieves	Aldrich	N.A.	N.A.
BTS cat	BASF	N.A.	N.A.

investigated conditions (-73 to 23°C and 17 to 550 bar) coincide only to a limited extent with typical conditions in our polymerizations. At the University of Pittsburgh, Mizan et al. (1994) investigated both dynamic and equilibrium data of the system at different temperatures. They showed the relatively slow reaching of equilibrium in the system, and, for the overlapping temperature (293 K), a good agreement with the data of Williams and Katz. We will compare literature data with our own experimental data, and will describe the data with a suitable EOS.

In this article we describe the setup for carrying out catalytic polymerizations in liquid propylene and show the calculation method for the determination of the polymerization kinetics. The system was used for the determination of the influence of a prepolymerization step, and the polymerization temperature on polymerization kinetics. Because of the fact that the hydrogen concentration at the active site is an important factor here, the VLE of this system was described using the Peng Robinson (PR) equation of state (EOS), after fitting these equations to experimental data obtained from polymerization.

Experimental Studies

Chemicals

The propylene used in the experiments was of so-called "polymer grade" and obtained from Indugas, with a purity $>99.5\%$, with propane as the main impurity. The hydrogen and nitrogen used were of $>99.999\%$ purity. Table 1 shows the different chemicals used, their origin, the purity, and the finishing purification steps. The hexane added to the system was of "Pro Analysi" quality obtained from Merck.

The hydrogen, nitrogen, and hexane were extra purified by passing them over a reduced BTS copper catalyst and subsequently through three different beds of molecular sieves, with pore sizes of 13, 4 and 3 angstrom, respectively. The BTS catalyst was obtained from BASF. The propylene was purified in the same way; additionally, it was led through a bed of oxidized BTS catalyst to remove CO.

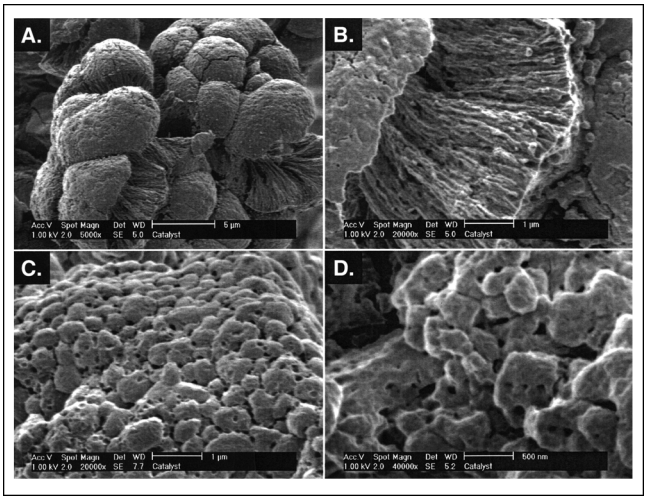

Figure 1. Electron microscopy pictures of the catalyst particles.

It is clear that the system is highly porous, with an average pore size of the macropores around 0.1 micron.

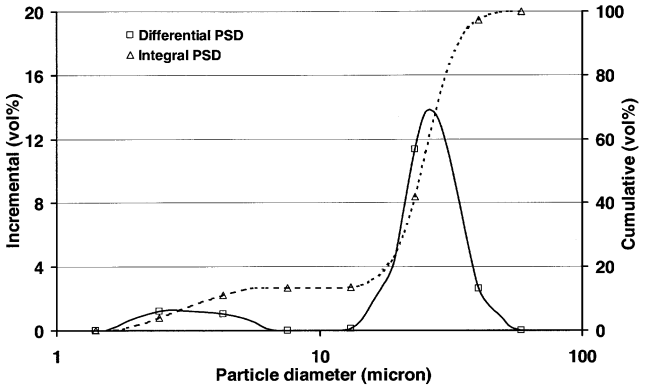

Figure 2. Particle-size distribution of the catalyst.

The average particle size is about 25 micron.

Catalyst System. The catalyst system that was used in the present work was a commercially available Ziegler-Natta catalyst of the fourth generation as defined by Moore (1996), with $TiCl_4$ on a $MgCl_2$ support. Triethylaluminum was used as a cocatalyst and the so-called D-donor (di-cyclopentyl dimethoxy silane) was used as external electron donor for regulation of the stereospecificity. Figure 1 shows electron microscopy (SEM) pictures of the highly porous catalyst material. It can be seen that the catalyst particles are composed of 20 to 30 spherically shaped subparticles. The particle-size distribution of the bare nonactivated catalyst is shown in Figure 2. The relatively narrow particle-size distribution shows an average particle diameter of 24.4 micron.

Experimental setup

Polymerization Reactor. The reactor system used in the present work was a 5-L stainless steel jacketed batch reactor obtained from Büchi (*Büchi BEP 280*), which is suited for operating pressures up to 40 bar. The batch reactor (indicated with I in Figure 3) is fitted with an overpressure valve and a rupture disk. The autoclave is equipped with a 6-blade turbine stirrer, mounted on a hollow stirrer shaft.

Small holes at the side of the shaft, near the turbine blades and in the reactor's gas cap, provide a recirculation of the gas through the liquid phase. Electronic pressure gauges and thermocouples are used to measure reactor pressure and temperature.

A cascade PID controller (II in Figure 3) was used to control reactor temperature. Water with a temperature of about 5 K above the reactor temperature set point was mixed with a varied amount of cold water (temperature about 15–20°C). The amount of cold water added was controlled by the two control loops having reactor temperature and jacket temperature as a process variable for the master and slave loop, respectively. This temperature control system allowed us to keep the reactor temperature within narrow boundaries of ± 0.2 K.

For safety reasons, the complete setup was placed in a concrete bunker and completely controlled from outside the

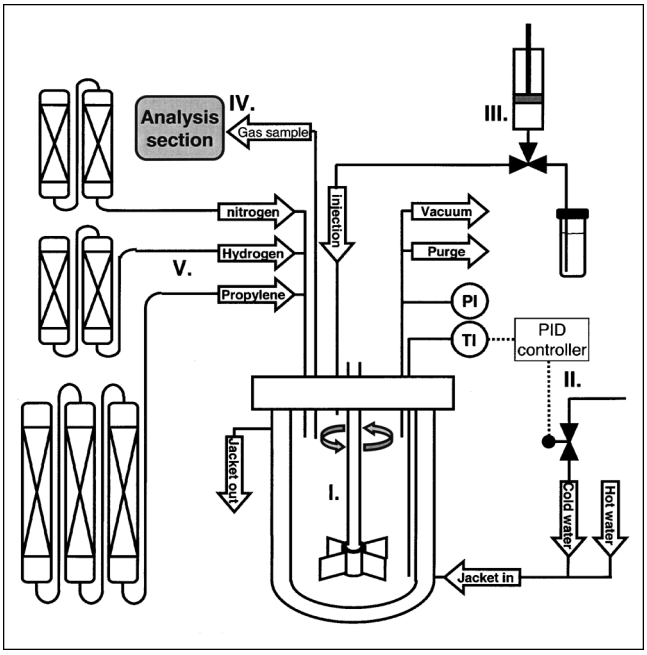

Figure 3. Polymerization setup.

I. 5-L autoclave reactor; II. PID-temperature control system; III. catalyst injection system; IV. analysis section, using GC and IR-analyzers; V. gas supply system with gas purification systems.

bunker. A control PC, running a program that was developed for this setup in HPVEE, was connected to a central data acquisition unit (*Hewlett Packard 3852A DACU*). All incoming data from mass-flow controllers, thermocouples, and pressure gauges is managed by this DACU and sent to the PC. All control actions from the PC to mass-flow controllers and valves follow the opposite route. Valves are controlled by actuators that are operated with pressurized air to prevent sparks from electrical switches.

The pneumatic injection system (III) allows the introduction of liquids and slurries into the reactor without contamination with impurities, even at high reactor pressures. The needles of the system are flushed with nitrogen continuously to prevent trapping of air when attaching the catalyst vials to the system.

Reaction Rate Measurements. The reaction rate of the highly exothermal polymerization reaction was measured by means of a calorimetric method, based on the heat balance of the reactor. Samson et al. (1998) described the principles of this measuring method, however, with respect to the method they used, some refinements were applied. Here, the thermal balance of the reactor is represented by

$$C_w \frac{dT}{dt} = C_1\left(\overline{T}_j - T_r\right) - Q_{BL} + Q_r \qquad \text{(J/s)} \qquad (6)$$

with the lefthand side of the equation representing the heat accumulation in the system. For isothermal conditions, the lefthand side term is equal to zero. Of the cooling jacket, temperatures of incoming and outgoing water are measured. As the flow profile in the jacket is approaching a plug-flow type of pattern, the jacket temperature is taken as the average of the two values

$$\overline{T}_j = \frac{T_{\text{inlet}} + T_{\text{outlet}}}{2} \qquad \text{(K)} \qquad (7)$$

In Eq. 6, C_1 represents the product of the heat-exchanging surface area and the heat-exchanging coefficient. As these values are hard to determine, but assumed to be constant in time, they are treated as a constant.

Q_r in Eq. 6 represents the heat produced by the polymerization reaction and is the product of reaction heat H_r, reaction rate R_p, and the mass of catalyst used m_{cat}

$$Q_r = R_p H_r m_{\text{cat}} \qquad \text{(J/s)} \qquad (8)$$

The Q_{BL} term represents the interaction of the system with the environment, and all other additional heat inputs and outputs, such as stirrer dissipation, heat exchange with the heated lid, and so on. Later in this article we will focus more on the different terms in Q_{BL}, but because of the fact that this term is shown to be constant over time, both with or without reaction, it is determined without reaction. At isothermal conditions and with $R_p = 0$, Eq. 6 gives Q_{BL}

$$Q_{BL} = \left[C_1\left(\overline{T}_j - T_R\right)\right]_{\text{no reaction}} \qquad \text{(J/s)} \qquad (9)$$

This temperature difference can be measured without reaction, and will be referred to as ΔT_{BL}, and, assuming a constant C_1 over time during polymerization, the reaction rate can be expressed as

$$R_p = C_1 \frac{\Delta T_{BL} - \left(\overline{T}_j - T_r\right)}{m_{\text{cat}} H_r} \qquad \text{(g/g·s)} \qquad (10)$$

The reaction rate R_p is, therefore, proportional to the corrected temperature difference between the jacket and the reactor content. Samson et al. (1998) showed that the curve of this temperature difference coincides with the real reaction rate curve, which was based on GC measurements.

Figure 4 shows a typical plot of the reactor and jacket temperatures during polymerization. It can be seen that the cas-

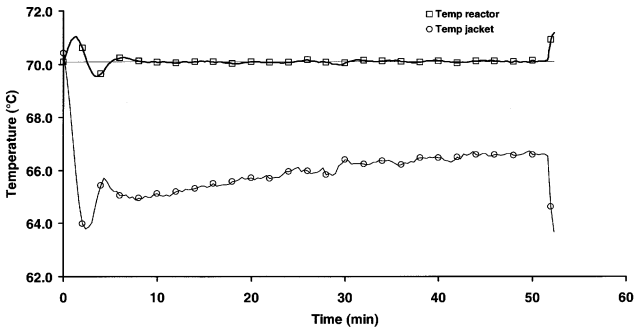

Figure 4. Typical temperature curves for a polymerization test in liquid propylene, at 70°C, in the presence of hydrogen.

The jacket temperature increases with time due to catalyst deactivation.

cade PID controller keeps the reactor temperature well within narrow boundaries (± 0.2 K). With decreasing catalyst activity, the temperature of the jacket increases. When translating this temperature plot towards a reaction rate plot, one can see that the reaction rate is oscillating in the initial stage due to oscillations of the PID control of the jacket temperature. In this stage, reaction rates indicated by this plot are, of course, not real reaction rates, as the system is not yet in isothermal operation. So, despite the fact that the system allows the measurement of polymerization rates with relatively high accuracy, it is not very suitable for measuring kinetics in the first 3 minutes of the experiment.

Sampling System. The setup is equipped with a sampling system that allows the operator to withdraw samples of the reactor content, in the present case a slurry of liquid propylene and polymer, during the polymerization run. The bottom valve of the system will open briefly and a sample of about 30 mL is withdrawn, without significantly disturbing the calorimetric measurements of the reaction rate. After closing the bottom valve, the sample is flashed in the sampling vessel and flushed with nitrogen to remove the monomer. During a run, several samples can be taken, as the minimum interval between two samples is about 10 min.

Gas Analysis. A heated pressure reducer valve is connected to the gas cap of the reactor, allowing the withdrawal of gas samples from the high-pressure reactor, without the risks of condensation in the sampling lines. Typically 40 Nml of gas is withdrawn from the reactor, and, because of the small amount, we can be sure that this does not significantly influence the composition of the reactor content. The pressure is reduced to a pressure of about 1.5 bar, led through a mass-flow controller and fed to a gas analysis section. This section comprises infrared analyzers to determine the ratio between the different monomers in the case of a copolymerization and a gas chromatograph to measure concentrations of the constant gases like nitrogen and hydrogen (indicated with IV in Figure 3).

Procedures

Catalyst Handling. The components of the catalyst system are prepared in a *Braun MB 150 B-G-II glovebox*, under a nitrogen atmosphere. Concentrations of oxygen and water are kept below a 0.1 ppm level. The catalyst, suspended in mineral oil, is weighed into a vial. The D-donor and aluminum alkyl are weighed into a separate vial in hexane dilution. The time between the contacting of the components—leading to complexation of the dimethoxysilane and the aluminum alkyl at room temperature—and injection of the mixture into the liquid propylene was kept constant at 15 min in all the tests. The conditions for the dispensing of the catalyst components are shown in Table 2.

Reactor Preparation. To purify the reactor for a polymerization, one can choose between two methods. Pickling—washing of the reactor with monomer and an aluminum alkyl at an elevated temperature—is often used to chemically clean the system. A disadvantage of this method is the nonreproducible amount of aluminum alkyl left behind this stage. A second possibility is to bake out the reactor at high temperatures, combined with evacuation and purging with a purified inert gas.

Table 2. Recipe and Conditions for Catalyst Component Addition

Component	Amount	Description
		Vial 1
$Al(Ethyl)_3$	270.0 mg	
Hexane	5 mL	Added at RT, to reduce $Al(Eth)_3$ concentration
D-donor	24.0 mg	Added at RT, contacted with $Al(Eth)_3$ for 15′ Injected in liquid propylene
		Vial 2
Oil	100.0 mg	
Catalyst	10.0 mg	In oil suspended catalyst is weight
Hexane	5 mL	Hexane is added to slurrify the catalyst Injected in liquid propylene, after injection Vial 1

In the present work the second method was used: the reactor was filled with nitrogen and evacuated during a period of 5 min. This was carried out at a wall temperature of 95°C and repeated for at least 5 times. After purifying, the reactor was brought to a pressure of 20 bars with hydrogen and kept for 10 min to check for gas leakage before evacuation.

Polymerization. After purification and evacuation of the reactor system, it was subsequently filled with the prescribed amount of hydrogen and 31.7 mole of propylene (1,334 gram or 2.6 L at 20°C). During polymerization, the impeller stirrer was used at 2,000 rpm and the reactor was heated to the required temperature. Then, the pre-contacted mixture of aluminum alkyl and D-donor was injected with 10 mL of hexane. The vial and injection system are flushed two extra times with 10 mL of hexane. When not using any form of prepolymerization, the catalyst suspension is subsequently injected and again the vial is washed twice with 10 mL of hexane. During polymerization, the reactor pressure and temperature are recorded, together with temperatures of incoming and outgoing cooling water of the jacket and the lid temperature.

To end the experiment, the unreacted monomer is flashed off by opening the vent valve. The reactor, initially at reaction temperature, will cool down due to this flashing. After flashing, the reactor is flushed several times with nitrogen to remove the last monomer. The powder is then taken from the reactor and dried overnight in a vacuum oven at 80°C. The reactor is washed out with a hydrocarbon, dried with pressurized air, and purified by using the method described above.

Prepolymerization. In the present work prepolymerization was carried out by reducing the polymerization temperature. When variations were to be made in the prepolymerization step, two types of prepolymerization are distinguished:

- *Fixed prepolymerization.* The temperature profile of a so-called fixed prepolymerization is shown in Figure 5a. The reactor is purified, filled with desired amounts of propylene and hydrogen and set to a constant, relatively low temperature, typically being 40°C. After reaching a constant reactor temperature, the catalyst components are injected into the reactor as described below and the reactor temperature is maintained at the prepolymerization temperature for a defined period of time, typically 10 min. After this prepolymer-

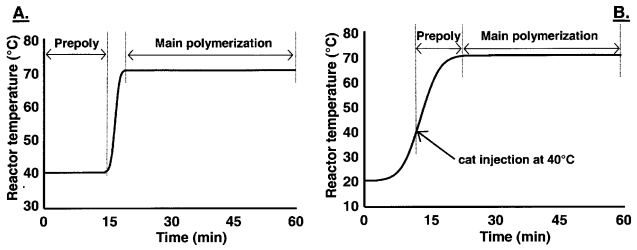

Figure 5. Two different prepolymerization methods used.

(A) The so-called fixed prepolymerization for 10 min at 40°C; (B) the nonisothermal prepolymerization, with, in this case, a catalyst injection at 40°C.

ization period, the reactor temperature is raised as quickly as possible to the temperature of the main polymerization. Heating of the system would normally take about 3 min.

• *Nonisothermal prepolymerization.* The temperature profile of a so-called nonisothermal prepolymerization is shown in Figure 5b. The reactor is purified and filled with the desired amounts of monomer and hydrogen and set to a constant low temperature, typically 20°C. Then, the pre-contacted mixture of aluminum alkyl and D-donor is injected into the system and, subsequently, the temperature of the reactor is raised to a final temperature of the main polymerization, typically 70°C. At a predefined moment during the heating of the reactor, the nonactivated catalyst is injected into the reactor system. This results in a short prepolymerization step at a nonconstant temperature. Varying the moment of injection of the catalyst can change the duration of the prepolymerization step and the reaction rate during prepolymerization.

Vapor-liquid equilibrium (VLE) measurements of propylene-H_2 system

Setup for Gas Analysis. To be able to measure the vapor-liquid equilibria in the hydrogen-propylene system under conditions comparable to those used in polymerization experiments, a *Varian 3300* gas chromatograph (GC) was used in combination with a *Hewlett-Packard 3392A* integrator. The GC was equipped with a 5 ft long HYSEP K column that was kept at 200°C in combination with a thermal conductivity detector. Nitrogen was used as a carrier gas.

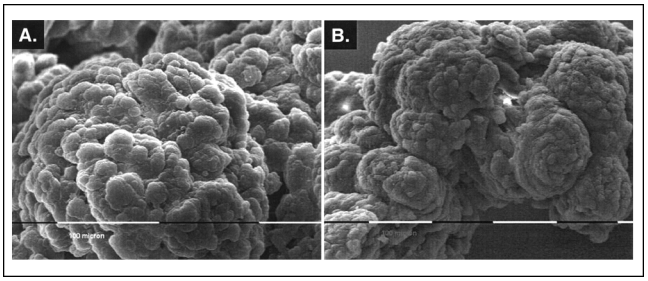

Figure 6. SEM of two powders yielding from different experiments under the same conditions.

No prepolymerization, T = 70°C, 0.21 mol H_2, 31 mol PPY.

Procedure for VLE. In the VLE measurements the batch reactor was prepared in the same way as described for the polymerizations. After flushing of the reactor with gaseous propylene, the system was evacuated. A known amount of liquid propylene was fed to the system, typically 31.7 mole. Then, by means of mass-flow controllers, the prescribed amount of hydrogen was added to the system and, subsequently, the system was brought to the desired conditions. Fully comparable to the polymerization tests, the reactor was equipped with the 6-blade turbine impeller at 2000 rpm.

20 min after reaching the desired process conditions, a small sample flow from the reactor was started, from which a gas sample was injected every 2 min into the GC column. In every batch at least five samples were analyzed. The integrator was used for evaluation of the GC-chromatograms. The number of counts in the peaks of the chromatogram was translated to numbers of moles using calibration data obtained with the same system. After analysis of the reactor gas, the temperature of the reactor was changed according to the new prescribed conditions and the analysis procedure was repeated.

Results and Discussion

Reproducibility

To be able to draw solid conclusions from the experiments, one has to be sure about the reproducibility with respect to powder morphology and the kinetic results of the polymerization reaction. Figure 6 shows the SEM pictures of two polymer samples, obtained in two different experiments under the same conditions. Both powders were produced in the presence of 0.21 mole of hydrogen, without a prepolymerization step, at 70°C. It can be seen that the reproducibility of the powder morphology is excellent. The same perfect reproducibility is observed in other duplicate polymerization tests.

Moreover, the kinetic results are reproduced to an acceptable degree. Figure 7 shows the kinetic curves of four different experiments. In experiments 1-1 and 1-2 the same recipes and procedures were used. It is clear that reproducibility is very good in this case; reaction rates vs. time are fully reproducible.

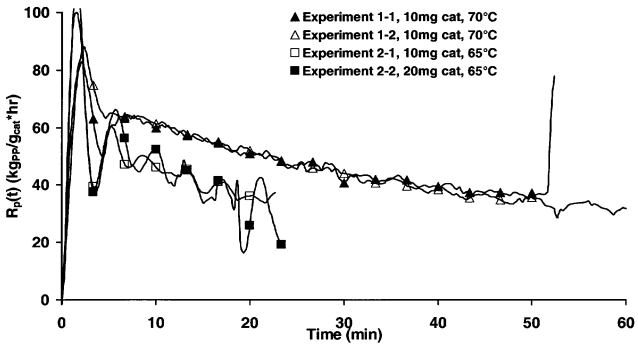

Figure 7. Two duplicated polymerization experiments.

Experiments 1-1 and 1-2 have the same recipe (10 mg of catalyst at 70°C), and experiments 2-1 and 2-2 used 20 and 10 mg of catalyst, respectively, at 65°C.

Since the amount of catalyst used in an experiment is not exactly the same in all experiments, the influence of changes is checked. In experiments 2-1 and 2-2, respectively, the normal and double amount of catalyst was used. It can be seen that the results of the tests are very similar and, thus, variations in catalyst amount (in experiments maximum up to 15%) do not influence results.

Determination of kinetic parameters

Determination of the Kinetic Parameters $R_{p,0}$ and k_d. In literature, the complicated kinetics of the multisite Ziegler-Natta catalysts are often dealt with by lumping the kinetic constants of the different types of active sites together or into a reduced number (for example, three sites, like Shimizu et al. (2001)) of kinetic parameters. For example, assuming the propagation constant does not depend on the length of the growing polymer chain, and assuming one overall propagation parameter for all sites, reduces the numerous propagation constants to one. The same is done for the different deactivation processes: when taking all deactivation processes into one combined empirical deactivation constant, the system is dramatically simplified. When one tries to refine the kinetic model by including kinetic behavior of the different sites of the multisite catalyst, it would be necessary to comprise more experimental data of another origin like MWD data. This will increase the number of parameters in the model significantly, and it is well known that measurement of the MWD is very hard to do in a quantitative manner.

In general, one can describe the rate of polymerization as a function of the concentration of active sites C^*, the concentration of the monomer at these centers $C_{\mathrm{PPY,site}}$, and the overall propagation constant k_p

$$R_p = k_p \cdot C_{\mathrm{PPY,site}}^{q} \cdot (C^*)^r \qquad (\mathrm{kg_{PP}/g_{cat}\cdot h}) \qquad (11)$$

with q and r being the orders of the reaction rate in monomer concentration and concentration of active centers, respectively. Due to diverse deactivation processes, the number of active sites can decrease in time. Weickert et al. (1996b) propose a list of possible mechanisms for real and apparent deactivation. In the measurements presented here, it is clear that activation of the catalyst is very fast, that is, at least faster than the time needed to reach the thermal equilibrium needed to determine the actual reaction rate. When assuming that the activation of the catalyst is instantaneous, the concentration of active sites will be maximum at $t = 0$. When lumping the rate constants of the various deactivation processes into one single parameter k_d, the decrease of the number of active sites will then be described by

$$-\frac{dC^*}{dt} = k_d \cdot (C^*)^p \qquad (\mathrm{mol/g_{cat}\cdot h}) \qquad (12)$$

Of course, the reasons for real or apparent deactivation are numerous and, when fitting experimental curves with equations based on Eq. 12, one might calculate low active sites concentrations even when low reaction rates are caused by other processes.

Equations 11 and 12 can be combined, and integrated for isothermal conditions to a general description for a reaction rate depending on time. When assuming a first-order deactivation, and first-order dependence of the reaction rate on monomer and active site concentration, this integration leads to

$$R_p = R_{p,0} \cdot e^{(-k_d \cdot t)} \qquad (\mathrm{kg_{PP}/g_{cat}\cdot h}) \qquad (13)$$

In this equation the complete reaction rate-time curve can be described by two parameters, being the initial reaction rate $R_{p,0}$ (fully activated catalyst, without any deactivation) and the deactivation constant k_d which is independent of the polymerization rate.

The two empirical kinetic parameters k_d and k_p can be assumed to depend on polymerization temperature according to Arrhenius

$$k_p = k_{p,0} \cdot e^{\left(\frac{-\mathrm{E_{act,p}}}{\mathrm{RT}}\right)} \qquad (\mathrm{m^3/h\cdot mol}) \qquad (14)$$

and

$$k_d = k_{d,0} \cdot e^{\left(\frac{-\mathrm{E_{act,d}}}{\mathrm{RT}}\right)} \qquad (\mathrm{h^{-1}}) \qquad (15)$$

After the experiment, the thermal data from the reactor and cooling jacket can be translated into a kinetic plot using the method described above. Next, this plot can be fit with the general description of the kinetics from Eq. 13, to quickly extract the basic kinetic parameters $R_{p,0}$ and k_d.

By plotting the natural logarithm of the reaction rate as a function of time, a linear fit can be made resulting in the deactivation constant, from the slope of the fit and the natural logarithm of the initial reaction rate, from the intercept at the y-axis. This standard and well-known method becomes clear from Figure 8.

Influence of "Base Line-Correction." As indicated in the experimental description, reaction kinetics are determined by evaluation of the temperature difference between the reactor contents and the cooling jacket in the isothermal operation.

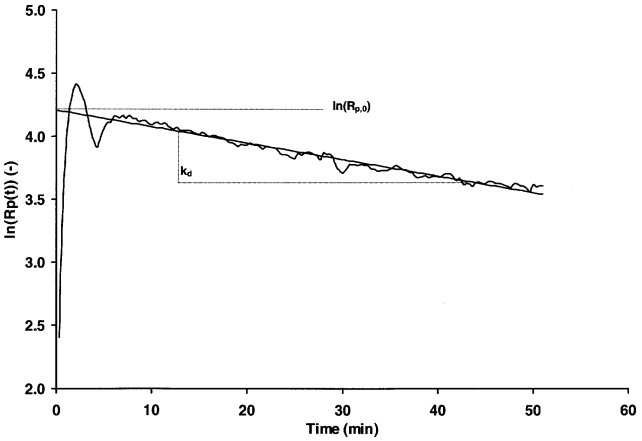

Figure 8. Determining initial reaction rate $R_{p,0}$ and deactivation constant k_d by plotting the natural logarithm of reaction rate vs. time.

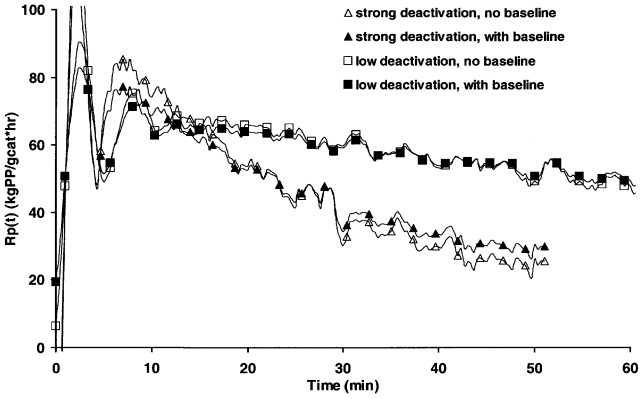

Figure 9. Changes in kinetic profile by neglecting the "base line" in experiments with different deactivation.

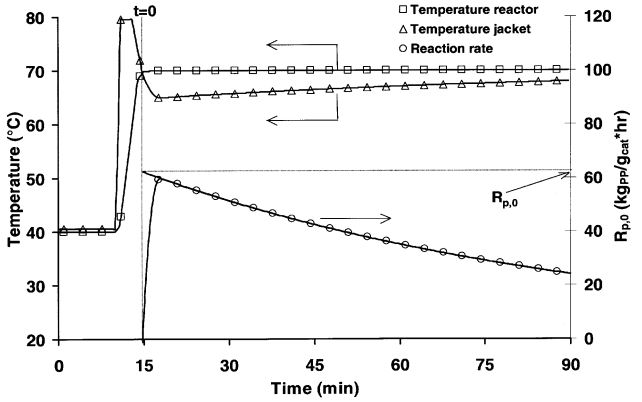

Figure 10. Interpretation of temperature information for an experiment with fixed prepolymerization step and the difficulty in definition of $t = 0$.

The method interprets this temperature difference as a linear measure for the amount of heat produced. However, when a polymerization experiment at 70°C is considered, one will see that before injection of the catalyst, the jacket temperature exceeds the reactor temperature due to the heat loss to the surroundings. A "negative" temperature difference is the result and direct interpretation of the temperature difference in terms of reaction rates, as was proposed earlier (Samson et al., 1998), can give problems. Therefore, it will be necessary to include the negative temperature difference between the reactor and the jacket in the case without polymerization in the evaluation. Figure 9 shows the effect of neglecting this temperature difference in the calculations. It will be clear that the extent of this effect will increase with increasing deactivation; the effect will be zero when no deactivation occurs. It will also increase with decreasing total heat production rate: at high reaction rates or large amounts of catalyst ($\Delta T_{BL}/\Delta T_{exp}$ is small), the effect becomes negligible, as heat loss to surroundings can be neglected with respect to heat production in polymerization. In the experiments shown in this work, corrections for this base line effect have been made, by adding the base line temperature difference ΔT_{BL} to the temperature difference measured in the experiment T_{exp}.

Extrapolation of Reaction Rate: Comparison Cases with and without Prepolymerization. Determination of the initial reaction rate, the $R_{p,0}$ value, is done by extrapolation of the reliable values for reaction rate—$R_p(t > 5$ min)—back to $t = 0$. This will yield reliable values for $R_{p,0}$ because $t = 0$ is well defined, the catalyst is activated almost instantaneously, and catalyst deactivation is negligible in this short initial stage. The ΔT curve of the first minutes after catalyst injection is useless to directly calculate reaction rates. As can be seen in Figure 4, the sudden heat production directly after catalyst injection causes the jacket temperature to fluctuate, although reactor temperature is rather stable (within 0.5 K). The calorimetric method can, as said before, only be used for isothermal conditions. The extrapolation method leads to a reliable and highly reproducible value for $R_{p,0}$.

In the case when a prepolymerization step is used, the reactor is prepared at a low temperature, typically 40°C, the alkyl-donor mixture is injected, and, finally, the catalyst is injected. Injection of the catalyst will start the prepolymerization reaction. Normally, reaction rate in the prepolymerization phase is not determined, but the reaction rate in the main polymerization phase is. Using the method described before, finding a value for the deactivation constant in the main polymerization stage is not a problem. The problem starts with the definition of $t_{main} = 0$ to find the value for $R_{p,0,main}$. Typically, the moment when $T_{jacket} < T_{reactor}$ is defined as $t_{main} = 0$. However, it is clear that, when comparing $R_{p,0}$ values of the cases with and without a prepolymerization step, one has to be careful. Especially in the case of a relatively strong deactivation, the choice for $t = 0$ will significantly influence the $R_{p,0}$ value. The $R_{p,0}$ value does not represent the "intrinsic" initial reaction rate. The problem is shown in Figure 10.

In addition, to transform the ΔT-curve with the polymer yield into a reaction rate curve, we have to take into account the amount of polymer produced during the prepolymerization step. This amount can be estimated when reaction kinetics without prepolymerization are well known. With these known kinetics, one can integrate the temperature-dependent reaction rate over prepolymerization time to obtain a reasonable estimation of the amount of polymer produced in this stage. In the prepolymerization experiments, such a calculation was performed.

Influence of the Heating of Reactor Lid. The reactor lid is heated by a separate heating system by means of water. The temperature of the lid is kept 2 K above the target reactor temperature, to reduce condensation of large amounts of monomer at the lid during polymerization. This temperature difference will continuously introduce heat to the reactor, according to

$$Q_{lid} = (T_{lid} - T_{reactor}) \cdot U_{lid \rightarrow reactor} \cdot A_{lid} \qquad \text{(J/s)} \quad (16)$$

However, of course, this is not a problem as all terms in this relation will be constant under isothermal conditions. Therefore, the heat input by the lid is constant and is, thus, included in the "base line correction" described previously.

Influence of the Heat Introduced by the Stirrer. In standard correlations that exist for calculation of heat dissipation by

agitated tank reactors, the Reynolds number for the tank is correlated with the power number. The Reynolds number for the current system will be around $6 \cdot 10^4$, resulting in a correlated power number of about 5 (Perry and Green, 1998). This means that dissipated heat is about 7 W

$$N_{Re} = \frac{D_a^2 N \rho}{\mu} = 6 \cdot 10^4 \Rightarrow N_p = 5 = \frac{g_c P}{\rho N^3 D_a^5} \Rightarrow P = 7 \text{ W} \quad (17)$$

In the conversion window within which we are working, the changes in viscosity are very small. Samson et al. (1998) showed that when going to conversion above 35%, problems occur with maintaining a well-stirred tank with the current agitator and, therefore, high conversions are to be avoided. Therefore, in the isothermal operation of this system, heat input by the stirrer is constant in time and, therefore, fully taken into account with the "base line correction."

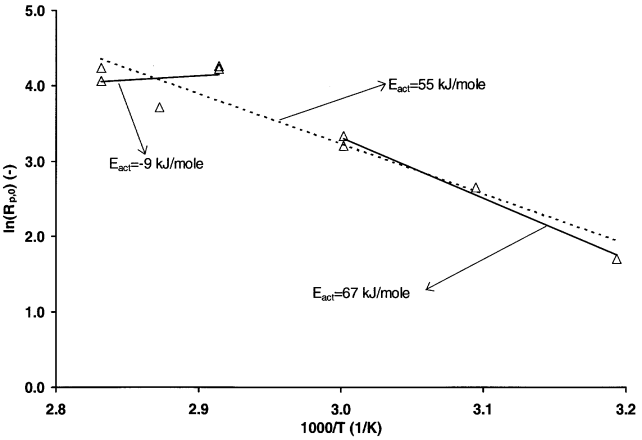

Figure 11. Arrhenius plot for initial reaction rates of experiments without prepolymerization step.

At high temperatures, reaction rate is not increasing with increasing temperature anymore.

Influence of temperature on polymerization kinetics

A series of experiments was performed to investigate the influence of temperature on polymerization kinetics. The recipes used in these polymerization experiments are shown in Table 3.

Figure 11 shows the Arrhenius plot of the extrapolated values of the initial reaction rate at the different temperatures, without applying a prepolymerization step. Temperatures were varied from 40 to 80°C. It is clear that the polymerization rate strongly decreases with decreasing temperature. However, at the higher polymerization temperatures, it seems that the temperature influence is significantly decreased. This is visualized by means of the three trend lines in the plot. The solid trend lines are linear fits (least squares) to the highest and lowest three temperatures, in the ranges 40–60°C and 70–80°C. The dotted line is the fit to all experiments. The respective activation energies calculated from these lines are given in the plot. The fit to the highest values gives even a negative value for E_{act} which, of course, does not have a real physical meaning.

This indicates that, at lower temperatures, the system is not mass-transfer limited. Typical activation energies for diffusion coefficients would be significantly lower than the values obtained here. However, the leveling off at higher temperatures is obvious. We can think of different explanations for this effect:

- Mass-transfer limitation is playing a role at higher reaction rates. It could be assumed that, at higher reaction rates, the system becomes mass-transfer limited, resulting in much lower activation energies. When considering the different steps in the monomer transport from bulk to active site, being convective transport to particle surface, convective transport through pores throughout the particle and transport by diffusion through the polymer from pore to active site, the diffusion part could become a transport limitation. However, the value for E_{act} determined for the 70 to 80°C interval seems to be even smaller than zero. Reaction rate does not increase with temperature anymore.

- At high initial reaction rates, the larger catalyst particles are deactivating due to overheating. As the particles are not prepolymerized before injection, the high initial rates can result in overheated particles.

To be able to check both hypotheses, one should use a prepolymerization step before the main polymerization. Results of this check are shown below.

In addition, the deactivation constants resulting from these experiments were plotted against polymerization temperature, as shown in Figure 12, indicated with the triangle shaped markers. Although correlation between deactivation constant and polymerization temperature is not as obvious as for $R_{p,0}$, it is clear that deactivation increases with increasing polymerization temperature. Difficulty in the determination of the temperature dependency is the fact that the value for k_d is sensitive for small changes in the experimental data. Although the R_p is highly reproducible for the different experiments, the deactivation constant fluctuates as a cause of the way it is determined. The activation energies determined for

Table 3. Polymerization Conditions

	Recipe				Pre-polymerization		Main Polymerization	
Type	Cat (mg)	Al/Ti (mg)	Al/Si (mg)	H_2 (mol)	T_{prepol} (°C)	Dur (min)	T_{main} (°C)	Dur (min)
None	10	270	24	0.22	—	—	70	75
Fixed	10	270	24	0.22	40	10	70	65
NIPP	10	270	24	0.22	various	various	70	±70

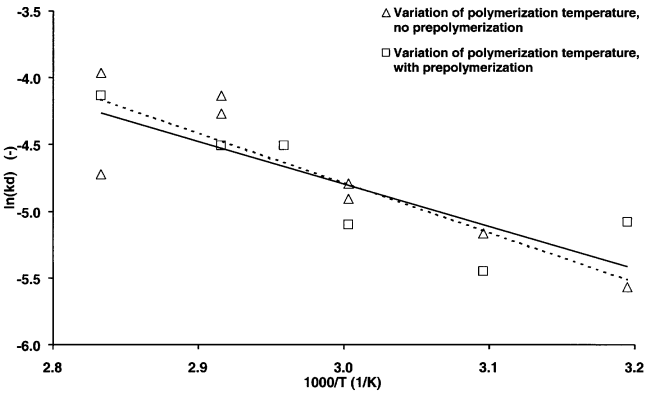

Figure 12. Arrhenius plot for the deactivation constant k_d.

The triangle shaped markers indicate the experiments without a prepolymerization step, and the square shaped markers indicate experiments with a fixed prepolymerization.

the combined deactivation processes are 31 and 27 kJ/mole with and without prepolymerization, respectively, as indicated by the dotted line in Figure 12.

Influence of prepolymerization on polymerization kinetics

A series of experiments was carried out using the so-called fixed prepolymerization. In this series, the catalyst was injected into the liquid propylene at a temperature of 40°C. The catalyst was prepolymerized for 10 min, then the temperature was raised to the target temperature. The results of this series are shown in Figure 13. The temperatures used in the Arrhenius plot are the temperatures during the main polymerization. Of course, again with decreasing temperature, the reaction rate in the main polymerization is decreasing. Again, the dotted trend line is fit to the full temperature range from 40 to 80°C, the solid line leaves out the highest temperature. It is clear that in the case of a prepolymerization, even at the highest temperatures for main polymerization, the reaction rate in the latter keeps increasing with increasing temperature. The prepolymerization step seems to solve the problem demonstrated in Figure 11. This is a strong indication that the reason for limitation at the highest reaction rate, as described before, is a result of thermal runaway on particle scale. A fraction of the catalyst, most probably the fraction with the largest particles, is deactivating due to overheating when a prepolymerization step is not applied. Starting the reaction at a lower rate, slowly increasing the outer surface area of the particle, and going to the high reaction rates after that, prevents the particle from runaway.

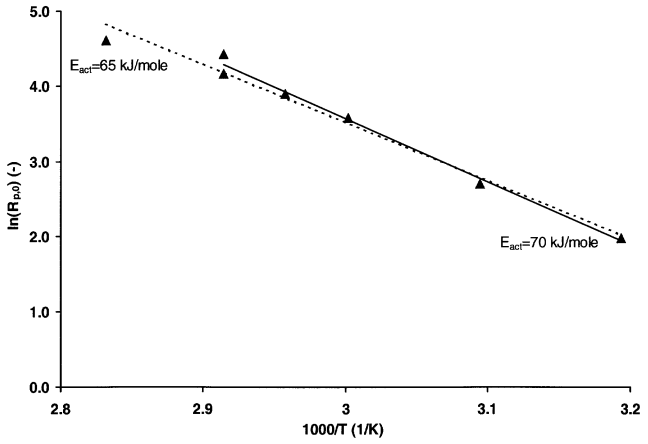

Figure 13. Arrhenius plot for initial reaction rates of experiments with fixed prepolymerization step.

Reaction rate increases here with polymerization temperature over the whole temperature range.

The deactivation behavior during the experiment is indicated by the square-shaped markers in Figure 12. Again, the k_d values increase with increasing temperature, and again the spread in values is larger than for $R_{p,0}$ values. The activation energy determined for the combined deactivation processes is about the same as without prepolymerization: 27 kJ/mole.

Influence of evaporation on powder morphology

When correlating powder properties such as particle-size distribution, bulk density, and SEM observed morphology to reaction conditions, one has to be sure that any morphological changes resulting from polymer workup can be neglected. As described before, the experiment is usually stopped by flashing the nonreacted monomer. As the speed of flashing will depend on flow restriction in the vent lines and the initial reactor temperature and pressure, we cannot be sure that the flashing procedure will be fully reproducible in all experiments. To ensure the insignificance of this fact, some tests were done to check this influence. Four polymer powders were produced in fully comparable polymerization experiments, but with a different flashing procedure: flashing temperature and speed of the flashing were varied. Two different temperatures were used: 70 and 20°C. In the case of 20°C, the reactor was cooled down first, and then the flashing was started. In the case of "fast-flashing" a small reactor sample was taken by means of the sampling system and dumped to an open sampling vessel of a much larger volume. In this way, flashing time from reactor pressure to normal pressure is below 1 s. In the case of slow flashing, the reactor was vented over a strongly restricted vent line; venting took about 1 h in this case. The SEM pictures of the four powders produced this way are shown in Figure 14. It shows that no influence of the flashing procedure on the powder morphology can be observed. The powders shown in Figure 14 were tested in mercury porosity measurement and showed the same pore-size distributions also in the finer pore-size range. Powder morphology seems to be established before flashing, and is apparently stable enough not to be disturbed by the flashing at the typical yield in these experiments. Therefore, the powder morphology observed at the end of a polymerization experiment is fully the result of the experiment and the conditions during that experiment, not the result of its finishing. However, this may not be the case for the flashing of particles at low prepolymerization yields.

Vapor-liquid equilibria of propylene-hydrogen system

Different Equations-of-State. At five different temperatures and 3 different hydrogen concentrations, the gas com-

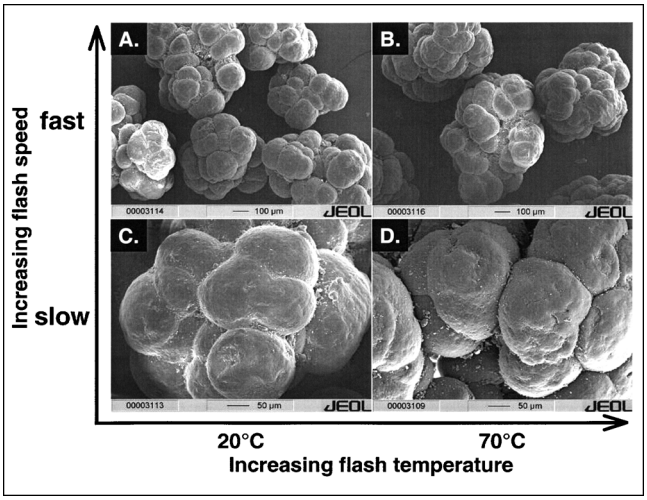

Figure 14. SEM of powders all produced at a standard polymerization experiment, but with varied flashing at end of experiment.

(A) Fast flashing at 20°C; (B) fast flashing at 70°C; (C) flow flashing at 20°C; and (D) slow flashing at 70°C.

position was measured without a polymerization reaction. In the measurements, the same amount of hexane was present as used in polymerization runs. The results of these equilibrium measurements are shown in Table 4.

To be able to describe the experimental data properly, *Hyprotech's HYSYS Plant 2.1* was used for equilibrium calculations. First, four different EOS-systems were used to describe experimental equilibrium data (Pater and Weickert, 2001), containing hydrogen mole fraction for both the liquid and gas phase of the binary system. The results of this fitting are shown in Table 5. In this table the deviation between the measured and calculated value is shown to demonstrate the performance of the calculation. Of course, the highest deviation indicates the worst result. It becomes clear that the Peng-Robinson and the sour-Soave-Redlich-Kwong are best able to describe the data. In the software package used, each

Table 4. Gas Chromatograph Measurements on VLE of the Hydrogen-Propylene System

	Experimental Recipe				Gas Chromatography	
Test No.	PPY (mol)	H_2 (mmol)	C_6H_{14} (mol)	T (K)	$(N_{H_2}/N_{PPY})_{gas}$ (mol/mol)	Y_{H_2}
1	31.73	68	0.423	294.1	0.03825	0.03680
2	31.73	68	0.423	313.9	0.02121	0.02080
3	31.73	68	0.423	323.7	0.01504	0.01480
4	31.73	68	0.423	333.8	0.01020	0.01010
5	31.73	68	0.423	343.7	0.00701	0.00700
6	31.73	223.2	0.423	295.4	0.11534	0.10340
7	31.73	223.2	0.423	314.2	0.07025	0.06560
8	31.73	223.2	0.423	323.9	0.05289	0.05020
9	31.73	223.2	0.423	333.9	0.03909	0.03760
10	31.73	223.2	0.423	343.7	0.02845	0.02770
11	31.73	637.9	0.423	293.3	0.34379	0.25580
12	31.73	637.9	0.423	313.3	0.20651	0.17120
13	31.73	637.9	0.423	323.6	0.15869	0.13700
14	31.73	637.9	0.423	333.8	0.12008	0.10720
15	31.73	637.9	0.423	343.8	0.09161	0.08390

Table 5. Fitting of Experimental Data Set (Pater and Weickert, 2001) for X_{H_2}/Y_{H_2} at Various Temperatures and Hydrogen Concentrations, Using Different EOS's

EOS	Interaction Parameter	Deviation
sour-Soave-Redlich-Kwong	Fixed: 0.00000	0.113
Soave-Redlich-Kwong	Fixed: 0.00000	0.179
Peng-Robinson	Fixed: −0.10360	0.115
sour-Peng-Robinson	Fixed: −0.10360	0.115
Peng-Robinson	IP = f(T)	0.033

EOS is using its own, fixed interaction parameter. To further improve the fit of the data, the optimal interaction parameter was determined for every temperature, from 30 to 80°C, using PR EOS. The following empirical relation describes the temperature dependence of the interaction parameter

$$\mathrm{IP} = 7.524\times10^{-4}\cdot T^2 - 0.4829\cdot T + 77.0879 \qquad (18)$$

where IP is the interaction parameter and T is the temperature in Kelvin. Table 5 shows the results of the use of the interaction parameters in Peng-Robinson. It is clear that the fit has improved to a large extent. The interaction parameter, as described in Eq. 16, used in the Peng-Robinson EOS gives an accurate relation to describe the H_2-PPY vapor-liquid system.

The now formed system of the Peng-Robinson EOS, with the temperature-dependent interaction parameter, was used to calculate the gas-phase composition in the polymerization reactor, for the conditions used in the tests in Table 4. Figures 15 to 17 show the results for low, medium and high hydrogen concentrations, respectively, in the system. In all cases results calculated with the fixed HYSYS interaction parameter and the results calculated with the temperature-dependent interaction parameter were compared for the situation with and without the presence of *n*-hexane. From these figures, it is shown that gas-phase hydrogen mole fractions are

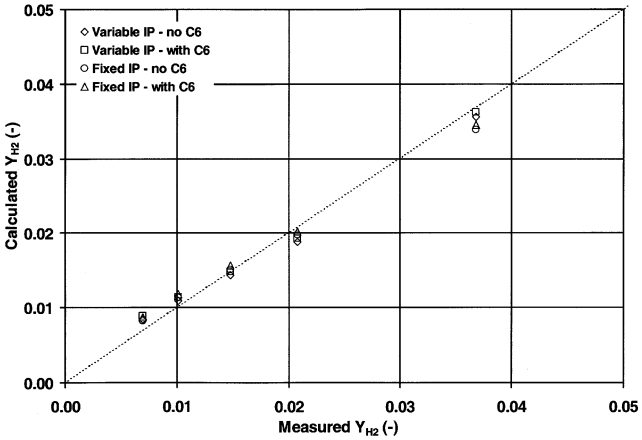

Figure 15. Measured mol fraction of hydrogen in gas phase, vs. the calculated mol fraction in gas phase, when adding 0.069 mol of H_2 to the reactor.

Calculation with Peng-Robinson using different settings.

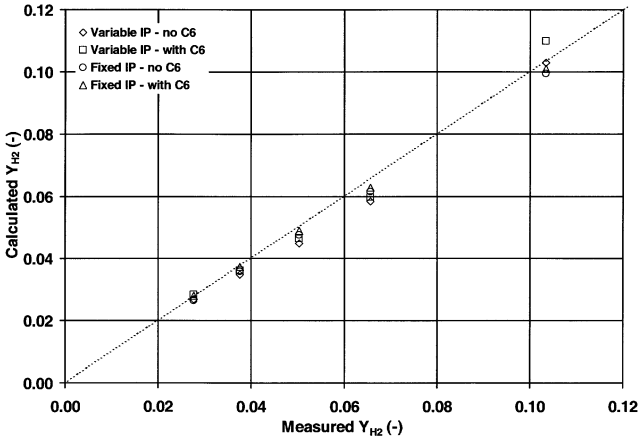

Figure 16. Measured mol fraction of hydrogen in gas phase vs. the calculated mol fraction in gas phase when adding 0.225 mol of H_2 to the reactor.

Calculation with Peng-Robinson using different settings.

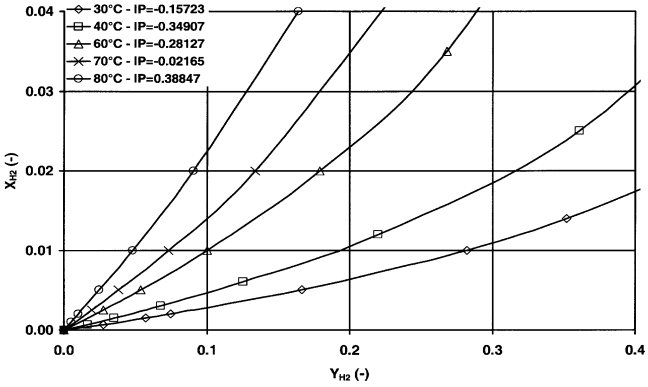

Figure 18. Mol fraction of hydrogen in liquid propylene, as a function of the mol fraction hydrogen in gas phase at a different temperature, calculated using Peng-Robinson EOS, with a varied interaction parameter.

well predicted with the chosen EOS. Figure 18 shows the direct relation between hydrogen mole fraction in the gas phase and in the liquid phase for typical temperatures used in these polymerizations. These graphs are used to convert GC measurements to hydrogen mole fractions in the liquid phase.

The five plots in Figure 18 can be well described by a second-order polynomial function in the form of

$$X_{H2} = AY_{H2}^2 + BY_{H2} \tag{19}$$

Table 6 shows, for the five temperatures used here, the values for A and B, best describing the relation between the compositions of gas phase and liquid phase.

In the next step, the HYSYS software was used to study the influence of variations in a few parameters that might not have been constant in the polymerization tests.

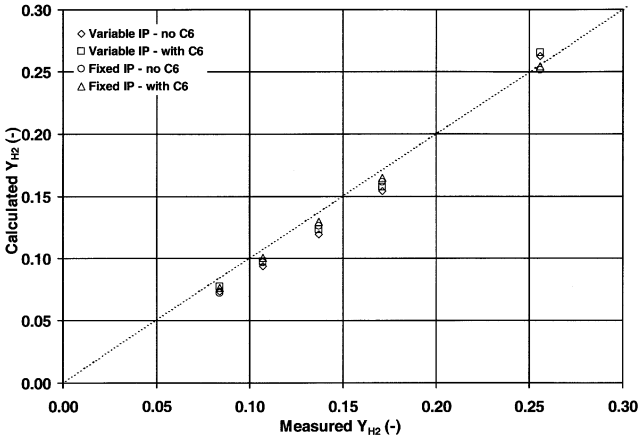

Figure 17. Measured mol fraction of hydrogen in gas phase vs. the calculated mol fraction in gas phase, when adding 0.655 mol of H_2 to the reactor.

Calculation with Peng-Robinson using different settings.

Influence of the Presence of Hexane. As will be described in part 2, in polymerization experiments the different catalyst components are injected as slurry or solution in hexane. Typically, two vials are used (the first containing the alkyl-donor mixture in hexane, the second containing the catalyst in hexane) containing 10 mL of hexane. After the injection of the separate liquids, the vial and injection system is always washed twice with 10 mL of fresh hexane. The use of this procedure leads to the introduction of about 60 mL of hexane in the reactor. As this amount is probably not completely constant in all tests, its influence on the gas-liquid equilibrium is investigated by using the calculation described before.

Table 7 shows the results of these calculations. It is clear that there is an influence of the variation in hexane concentration on hydrogen concentrations, but the influence is minor. The percentage in Y_{H2} goes up to 4.4% (corresponding change in X_{H_2} of 3.2%) at the highest temperatures, but this applies to deviations of 30% in the amount of added hexane. As in normal experiments, a maximum variation of 10 mL in the amount of added hexane can be expected, changes in H_2 concentration due to changes in hexane can be neglected.

Influence of the Presence of Nitrogen. In the preparation of a liquid pool polymerization, liquid monomer is transported from the central storage vessel, through the purification sections, towards the polymerization setup. Transport of the monomer is performed by using an overpressure of nitrogen of about 8 bars (pressure is kept around 18 bar at a temperature below RT). Due to the fact that the nitrogen will dis-

Table 6. Temperature-Dependent Coefficients for Calculating the Relation between Compositions of Gas Phase and Liquid Phase in Eq. 19

Temp. (K)	A	B	Temp. (K)	A	B
303	0.0616	0.01807	343	0.2842	0.11184
313	0.1560	0.01529	353	0.3193	0.19174
333	0.2952	0.05301			

Table 7. Y_{H_2} and X_{H_2} at Different Hexane Concentrations and Temperatures, Calculated with Peng-Robinson EOS, Using Temperature-Dependent Interaction Parameter*

C_6	30°C		60°C		80°C	
(mL)	Y_{H_2}	X_{H_2}	Y_{H_2}	X_{H_2}	Y_{H_2}	X_{H_2}
Low Hydrogen (0.069 mol)						
40	0.0267	0.0007	0.0115	0.0010	0.0066	0.0012
50	0.0268	0.0007	0.0116	0.0010	0.0067	0.0012
60	0.0269	0.0007	0.0116	0.0010	0.0068	0.0012
70	0.0270	0.0007	0.0117	0.0009	0.0069	0.0011
Moderate Hydrogen (0.23 mol)						
40	0.0835	0.0022	0.0371	0.0032	0.0217	0.0039
50	0.0837	0.0022	0.0373	0.0032	0.0220	0.0039
60	0.0837	0.0022	0.0375	0.0032	0.0223	0.0038
70	0.0842	0.0022	0.0378	0.0032	0.0226	0.0038
High Hydrogen (0.66 mol)						
40	0.2050	0.0063	0.0983	0.0092	0.0595	0.0112
50	0.2054	0.0063	0.0988	0.0092	0.0603	0.0111
60	0.2060	0.0062	0.0994	0.0091	0.0611	0.0110
70	0.2065	0.0062	0.1000	0.0091	0.0619	0.0109

*N_2 is assumed to be absent.

solve in the propylene, a variable amount of nitrogen is introduced in the polymerization reactor when filling it. The amount of nitrogen present in the propylene will depend on the storage temperature (the storage vessel is located outside, so the temperature will change with the season) and contact times. As a continuous amount of nitrogen present during polymerization is not guaranteed, the influence of this nitrogen presence was studied, using the Peng-Robinson EOS, with the temperature-dependent interaction parameter. Table 8 shows the result of these calculations. The influence of four different amounts of nitrogen on the hydrogen concentrations was evaluated. It is clear that this influence is very small. Both the X_{H_2} and the Y_{H_2} do not change more than 1% after adding 0.15 mole of nitrogen, the estimated maximum amount of nitrogen that can be present. This is checked by the pressure during the polymerization: from this the amount of nitrogen present in the system can be precisely calculated. From the results as presented in Table 8, it can be concluded that there is no need to precisely calculate the amount of nitrogen present in the system during polymerization experiments, as it does not influence the parameters important to the polymerization reaction itself.

Table 8. Y_{H_2} and X_{H_2} at Different Amounts of N_2 and Temperatures, Calculated with Peng-Robinson EOS using the Temperature-Dependent Interaction Parameter*

N_2	30°C		60°C		80°C	
(mol)	Y_{H_2}	X_{H_2}	Y_{H_2}	X_{H_2}	Y_{H_2}	X_{H_2}
Low Hydrogen (0.069 mol)						
0.00	0.0269	0.0007	0.0116	0.0010	0.0068	0.0012
0.05	0.0264	0.0007	0.0115	0.0010	0.0068	0.0012
0.10	0.0259	0.0007	0.0114	0.0010	0.0067	0.0012
0.15	0.0254	0.0007	0.0113	0.0010	0.0067	0.0011
Moderate Hydrogen (0.23 mol)						
0.00	0.0838	0.0022	0.0375	0.0032	0.0223	0.0038
0.05	0.0824	0.0022	0.0372	0.0032	0.0222	0.0039
0.10	0.0809	0.0022	0.0368	0.0032	0.0220	0.0039
0.15	0.0796	0.0022	0.0365	0.0032	0.0218	0.0039
High Hydrogen (0.66 mol)						
0.00	0.2060	0.0062	0.0994	0.0091	0.0611	0.0112
0.05	0.2037	0.0062	0.0985	0.0091	0.0607	0.0111
0.10	0.1997	0.0062	0.0976	0.0091	0.0603	0.0110
0.15	0.1967	0.0062	0.0967	0.0091	0.0599	0.0109

*For all calculations $V_{hexane} = 60$ mL is used.

Conclusions

A setup has been described for the polymerization of liquid propylene using typical industrial catalyst systems, which is a Ziegler-Natta catalyst here. In the determination of the polymerization kinetics, a calorimetric method was used, based on assumptions of isothermal conditions and a constant heat exchange between the reactor content and the reactor wall. It was shown in polymerization experiments that the interpretation method used so far could be improved in some details. This is especially important in tests with low heat production and in experiments showing relatively strong deactivation behavior of the catalyst.

Furthermore, it has been demonstrated that, at higher polymerization temperatures, the use of a prepolymerization step can increase the polymerization rate in the main polymerization stage. This effect is ascribed to the prevention of thermal runaway on particle scale when using this prepolymerization. The outer surface area of the particle is, thus, enlarged at a relatively low polymerization rate, before subjecting the particle to a high polymerization rate.

It has been shown that the Peng-Robinson EOS gives the best results for describing the binary system of propylene and hydrogen in a vapor-liquid equilibrium. The frequently used standard interaction parameter of -0.10360 for this system was not found to be the optimum. Here, a temperature-dependent interaction parameter was derived. Using this relation, the predictive power of the Peng-Robinson relation was strongly improved.

Applying the PR-EOS, with the temperature-dependent IP, equilibrium measurements based on the gas chromatograph analyses carried out using the polymerization reactor were described effectively. It was also shown that changes in the amount of nitrogen or hexane present in the liquid propylene polymerizations do not significantly change the parameters (like X_{H_2}) for important polymerization.

Acknowledgments

The work presented in this article was carried out in a cooperation with The Dow Chemical Company, Freeport, TX. The authors wish to thank Dow for both the financial and the intellectual input. In addition, the technical assistance of Gert Banis, Fred ter Borg, Karst van Bree and Geert Monnink is highly appreciated.

Notation

ΔH_r = heat of reaction, J/mol
A = surface area, m^2
C = concentration, kg/m^3
C_w = heat capacity, J/K
D_a = stirrer diameter, m
E_{act} = activation energy, J/mol
g_c = gravitational conversion factor
j = chain length
k = reaction rate constant
m = mass, g
N = impeller rotational speed, s^{-1}

N_P = power number
N_{Re} = Reynolds number
p = order of deactivation
p = pressure, bar
p^0 = normal vapor pressure, bar
P = power, J/s
Q = dissipated heat, W
q = chain transfer probability
r = order of reaction rate in C_m
R = gas constant, J/mol·K
R_p = rate of polymerization, kg/g·h
t = time, s
T (or $\bar{T}$) = temperature (average temperature), K
U = heat-transfer coefficient, J/s·m^3
X = mole fraction in liquid phase
Y = mole fraction in gas phase
y_j^d = differential mole weight distribution

Greek letters

μ = viscosity, Pa·s
ρ = density, kg/m^3
ϕ = volume fraction
χ = Flory-Huggins interaction parameter

Subscripts

BL = base line
cat = catalyst
d = deactivation process
gas = gas phase
H_2 = hydrogen
jacket = jacket
lid = reactor lid
liq = liquid
m = monomer
main = main polymerization stage
p = propagation process
POL = in the amorphous polymer
PPY = propylene
prepol = prepolymerization stage
r, reactor = reactor
site = at the active site
stirrer = stirrer

Abbreviations

DACU = data acquisition and control unit
D-donor = dicyclopentyl dimethoxy silane
EOS = equation of state
GC = gas chromatograph
IP = interaction parameter
MW = molecular weight
MWD = molecular weight distribution
PO = polyolefin(s)
PPY = propylene
PR = Peng-Robinson
RT = room temperature
SEM = scanning electron microscopy
SRK = Soave-Redlich-Kwong
VLE = vapor-liquid equilibria
ZN = Ziegler-Natta

Literature Cited

Meier, G. B., G. Weickert, and W. P. M. van Swaaij, "Comparison of Gas and Liquid Phase Polymerization of Propylene with a Heterogeneous Metallocene Catalyst," *J. Appl. Pol. Sci.*, **81**, 1193 (2001).

Mizan, T. I., J. Li, B. I. Morsi, M.-Y. Chang, E. Maier, and C. P. P. Singh, "Solubilities and Mass Transfer Coefficients of Gasses in Liquid Propylene in a Surface-Aeration Agitated Reactor," *Chem. Eng. Sci.*, **49**, 821 (1994).

Moore, E. P., *Polypropylene Handbook*, Hanser Publishers, Munich (1996).

Pater, J. T. M., and G. Weickert, "Experimental Equilibrium Data on the H_2-PPY System," internal report IPP Research group, Enschede, The Netherlands (2001).

Perry, R. H., and D. W. Green, *Perry's Chemical Engineers Handbook*, 7th ed., McGraw-Hill, New York, p. 18−12 (1998).

Samson, J. J. C., G. Weickert, A. E. Heerze, and K. R. Westerterp, "Liquid-Phase Polymerization of Propylene with a Highly Active Catalyst," *AIChE J.*, **44**, 1424 (1998).

Shimizu, F., J. T. M. Pater, G. Weickert, and W. P. M. van Swaaij, "Three-site Mechanism and Molecular Weight: Time Dependency in Liquid Propylene Batch Polymerization Using a $MgCl_2$-supported Ziegler-Natta Catalyst," *J. Appl. Pol. Sci.*, **81**, 1035 (2001).

Weickert, G., *Modellierung von Polymerisationsreaktoren*, Springer-Verlag, Berlin, pp. 16−59 (1996a).

Weickert, G., P. Roos, G. B. Meier, J. J. C. Samson, and K. R. Westerterp, "Kinetic Study of Gas Phase Polymerization of Ethylene with rac-$Me_2Si[Ind]_2ZrCl_2$/MAO Supported on Silica Gel," *Proc. meeting Working Party Polymerization Reaction Eng.*, Thessaloniki, Greece (1996b).

Williams, R. B., and D. L. Katz, "Vapor-Liquid Equilibria in Binary Systems. Hydrogen with Ethylene, Ethane, Propylene, and Propane," *Ind. Eng. Chem.*, **46**, 2512 (1954).

Young, C. L., "Solubility data. Hydrogen-Olefins Systems," *Sol. Data Ser.*, **5**, 400 (1981).

Manuscript received Sept. 21, 2001, and revision received June 12, 2002.